IEEE Access
Multidisciplinary | Rapid Review | Open Access Journal

Received December 24, 2019, accepted February 6, 2020, date of publication February 13, 2020, date of current version February 27, 2020.

Digital Object Identifier 10.1109/ACCESS.2020.2973672

Development of a Robotic Companion to Provide Haptic Force Interaction for Overground Gait Rehabilitation

HOSU LEE[1], AMRE EIZAD[2], SANGHUN PYO[1], MUHAMMAD RAHEEL AFZAL[3], MIN-KYUN OH[4], YUN-JEONG JANG[4], AND JUNGWON YOON[1], (Member, IEEE)

[1]School of Integrated Technology, Gwangju Institute of Science and Technology, Gwangju 61005, South Korea
[2]School of Mechanical and Aerospace Engineering, Gyeongsang National University, Jinju 52828, South Korea
[3]Department of Mechanical Engineering, KU Leuven, 3000 Leuven, Belgium
[4]Department of Rehabilitation Medicine, Gyeongsang National University School of Medicine, Gyeongsang National University Hospital, Jinju 52727, South Korea

Corresponding authors: Jungwon Yoon (jyoon@gist.ac.kr) and Min-Kyun Oh (solioh21@hanmail.net)

This work was supported in part by the National Research Foundation (NRF) of South Korea under Grant 2019M3C1B8090798, in part by the Ministry of Culture, Sports, and Tourism (MCST) and the Korea Creative Content Agency (KOCCA) through the Culture Technology (CT) Research and Development Program 2018, and in part by the Lee Jung Ja Research Grant of Gyeongsang National University Hospital under Grant LJJ-GNUH-2019-0003.

ABSTRACT The aim of gait rehabilitation is to achieve independent ambulation. Somatosensory augmentation with external haptic sources can improve the subject's ability to walk or stand. This paper presents the development and evaluation of a robotic system prototype that delivers haptic forces to aid overground gait rehabilitation. This portable system is based on a compact, mobile robot that is equipped with force and LIDAR sensors. The robot is flexibly linked to the user, which allows the force interaction between the user and machine to be halted when desired. During operation, the system can dynamically transition between modes in which force is applied or distance is maintained to emulate the experience of a human walking a dog on a leash. The haptic feedback from our system was evaluated in a pilot study that involved six young, healthy subjects and one individual recovering from a hemiparetic stroke. The study comprised independent and device-assisted walking trials. When using the device, the subjects walked continuously as it transitioned between distance and force modes. Gait speed and step length increased when force was applied and decreased as the force was removed. The improvements exhibited by an individual suffering from stroke were similar to those exhibited by healthy subjects. The application of haptic forces has a high potential for improving the efficiency of overground gait training with simple interactions.

INDEX TERMS Haptic interfaces, rehabilitation robotics, mobile robots.

I. INTRODUCTION

Individuals suffering from stroke typically regain some locomotor function but continue to exhibit significant gait deficits [1], [2]. Therefore, stroke survivors experience a loss of independence in terms of daily activities and restricted community ambulation, which limits their ability to engage in work, leisure, and social activities. Regaining the ability to walk independently is an important factor in the reintegration of stroke survivors [1], [3], [4]. Gait rehabilitation protocols are used to minimize the risks involved in increasing a patient's mobility; these involve exercises that instigate functional gait adaptations [5], [6] by subjecting the patient to varying physical demands. Gait adaptations that occur during rehabilitation extend into unassisted walking behaviors [7], [8]. The continuation of these gait adaptations is believed to be caused by the retention of adapted motor patterns by the central nervous system (CNS) after training has ceased [9].

Following a stroke, overground gait adaptation training is complemented by assistive devices and other therapies [10]. Individuals with a diminished sense of balance and weak sensorimotor systems encounter problems related to gait failure, which include an increased chance of falls, and a loss of independence. To overcome these problems, individuals must improve their sense of balance and gait ability through

The associate editor coordinating the review of this manuscript and approving it for publication was Jenny Mahoney.

the use of assistive devices [11], [12]. However, the fluidity of an individual's motion is restricted when common walking aids are used. Subjects have been observed to bend forward, put a considerable load on the assistive device, or reduce their gait speed [13]–[18]. Therefore, a number of researchers do not recommend the use of such devices for gait training [13]–[15].

In general, rehabilitation devices use multisensory stimuli [19]–[21] for task-oriented neuromotor rehabilitation following trauma [22]. Sensorimotor coupling is useful for rehabilitation as sensory inputs can be coupled with motor adaptation to enhance the spatiotemporal organization of movements [23]. Evidence shows that light, non-supportive contact with a fixed object can limit postural deviations during locomotion [24]–[27]. Furthermore, Afzal et al. observed that haptic cues delivered by a wearable device can emulate such contact, and effectively reduce the body sway of healthy subjects performing tasks while standing [28].

Specially trained rehabilitation dogs can be used as an alternative source of haptic cues for patients with chronic stroke symptoms. This concept originated from clinical observations [29] as subjects walking with trained service dogs exhibited better fluidity of gait and took longer steps than those supported by conventional walking aids. The use of rehabilitation dogs was evaluated in a pilot study of four individuals with stroke. All subjects exhibited an increased gait speed and improved gait pattern after three weeks of training [29]. To extend this concept, a recent study has measured the effects of haptic inputs delivered in the form of forward-leading tensile forces applied to the hand while patients were walking on a self-paced treadmill. It was found that the application of a leading force increased instantaneous gait velocity and step length [22]. Providing haptic inputs to a walking subject may alter trunk and whole-body motion and spatiotemporal gait parameters related to stability, muscle activity, and reflex modulation [30]–[32]. If haptic inputs have a positive effect on walking performance, they may also be effective tools for locomotor rehabilitation [33]. However, the kinematic and temporal gait parameters for a standard treadmill differ significantly from overground gait parameters [34]; and a standard treadmill does not provide the same voluntary walking experience. More complex adaptive treadmill systems can emulate a voluntary gait experience [7] and simulate an environment that is close to real-life walking when combined with immersive technologies [35]. Furthermore, users with limited balance function can be protected using suspended safety harnesses. However, overground gait training delivers a more realistic walking experience for patients with better balance function as obstacles and turns can be more easily introduced to stimulate multiple senses. Recovering stroke patients consume less metabolic energy [36] and improve their gait endurance [37] when walking on real ground rather than on a treadmill. Therefore, individuals with stroke that are capable of unassisted walking can benefit from the use of a system that enables overground gait training. Furthermore, a portable overground gait rehabilitation system is more accessible and therefore, may increase participation in long-term rehabilitation activities. Pyo et al. reported that the gait of a stroke survivor improved when the patient was walking with an instrumented cane that provided haptic cues [38]. In this context, haptic cues may be a useful therapy for intuitive interaction during overground gait rehabilitation; their suitability for post-stroke ambulation recovery can be explored further.

Inspired by these previous works, in this study, we present the design and evaluation of a companion robot that can provide haptic interaction in the form of a tensile force applied to the user's hand, for the purpose of overground gait training. The presented companion robot is based on the hardware layout developed by Pyo *et al.* [38], which was modified to simulate the haptic interaction between a human and dog walking together. The robot is equipped with force and LIDAR sensors that are used to determine haptic interaction forces and the distance between the robot and the user. The companion interacts with the user via a flexible fixed-length leash that is held by the user. The system can operate in a force mode in which the leash applies a force in the direction of motion, or in a distance mode in which a fixed separation is maintained between the user and companion without applying any substantial forces to the leash. The robotic companion is designed to combine the benefits of a robotic system and animal-assisted training while overcoming the limitations of existing works. Animal-assisted training is sometimes complicated by the unpredictable behavior of dogs as they are affected by environmental stimuli such as scents, sounds, and the presence of other animals or people. Some existing mechanical solutions require the use of a treadmill which may not be available or provide a suitably realistic experience. The performance of our system was evaluated by investigating the experience of healthy users and an individual recovering from stroke when haptic forces are delivered through the leash and following the removal of these forces. The design of the system is discussed in Section II, and the details of the pilot study are presented in Section III. The experimental results are provided and assessed in Section IV, and our conclusions are drawn in Section V.

II. SYSTEM DESIGN

A. THE PORTABLE HAPTIC FORCE SYSTEM CONCEPT

The system presented in this paper has been designed for use by individuals who are in the chronic stage of recovery after stroke and are capable of walking without assistance. Figure 1 shows the two simplified interaction modes between a human and dog when walking overground. The dog may walk at pace with the human so that there are no interaction forces between them. In this case, the dog maintains its distance from the human by matching its velocity with that of its human companion. Alternatively, the dog may try to increase its speed and pull on the leash so that the human experiences a tensile force acting on their hand. Although the leash is always in the human's hand, a force is only applied in the second case.

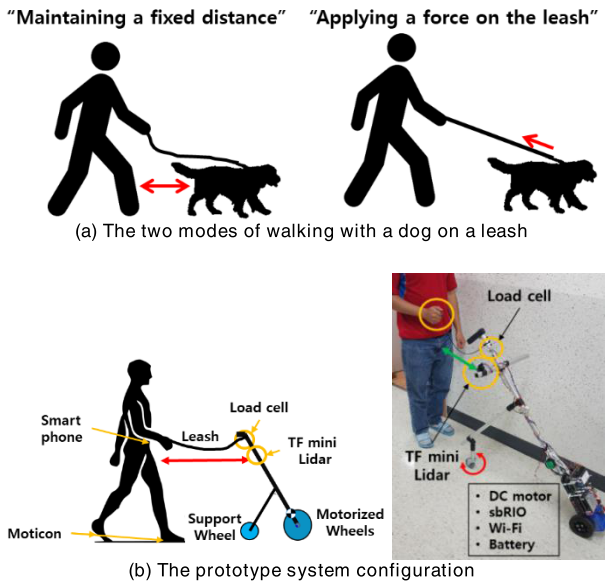

(a) The two modes of walking with a dog on a leash

(b) The prototype system configuration

FIGURE 1. The design of the prototype system.

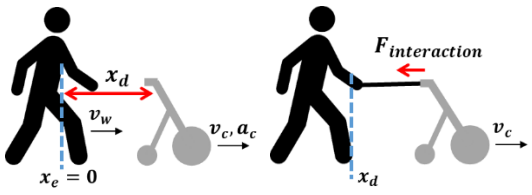

(a) Distance mode (b) Force mode

FIGURE 2. The two control modes of the prototype system.

We propose the use of a robotic companion that has a flexible haptic interface with the user and simulates these two states. Figure 1(b) shows the concept of our prototype robotic companion system. Walking without force interaction is simulated by the distance mode (as shown in Figure 2(a)), and walking with a constant force interaction is simulated by the force mode (as shown in Figure 2(b)). The target of this system is to deliver a force interaction with a controlled magnitude and duration at a specified time. The distance and force modes were implemented so that the system could controllably transition between the two modes.

In order for the robotic companion to operate in the two modes mentioned above, it requires a means of measuring the horizontal distance between itself and the user and a means to establish a flexible linkage with the user at hand level such that the force applied through it can be measured. In a previous work [38] we had developed a wheeled haptic cane. In order to provide removable haptic input at the hand during walking, we built upon this experience and designed a free-standing mobile robotic platform based on the haptic cane hardware layout. As shown in Figure 1(b), the hardware layout was modified by adding a caster wheel at the back so that there is ample support in the fore-aft direction to handle the forces generated by the flexible linkage. The caster wheel also allows passive turning. A special mounting assembly for the LIDAR sensor was also added that allowed for the easy placement of the sensor on the right or left side of the robot to ensure ease of adaptability for different users. The flexible linkage was attached in such a way that the force sensor built into the structure can be used to determine the horizontal force carried by the linkage. This particular design was developed because it allows for the easy mounting of the LIDAR sensor to measure the distance between the robot and the user's center of mass and also allows tensile force to be applied at the height of the user's hand. Although the system has a narrow wheelbase, all of the heavy components such as batteries, motor, etc. are placed very close to the ground resulting in a very low center of gravity (COG). The low COG and the added caster wheel ensure sufficient amount of stability according to the system's target ground conditions, i.e. flat, hard surfaces such as tiled floors, concrete pavement, tarmac, etc. Furthermore, a completely new software was developed to control the companion robot that implemented distance and constant force running modes and incorporated special algorithms for safe transitions between the modes. The details are given in the following parts of this section.

The human-robot interaction must transition between continuous and constant force, and no force. This may be achieved using a rigid linkage between the human and robot, but it is challenging to produce a zero-force sensation with such an arrangement. Therefore, the system presented here uses a flexible linkage similar to the leash used to walk a dog. A detailed description of the system hardware is given in Section II-D.

B. DESIGN OF THE CONSTANT-FORCE MODE

The low-level controller shown in Figure 3 controls the system speed while operating in both system modes. The low-level motor controller determines the system velocity through proportional-integral (PI) control. In the block diagram, v_d is the desired command input, v_c is the system speed feedback obtained from the motor encoder, ω_d is the desired wheel angular velocity, T_m is the torque input from the PI controller, θ_m is the actual angular velocity, T_D is the torque disturbance, and k_e is the gain used to convert the encoder rotation angle into system velocity.

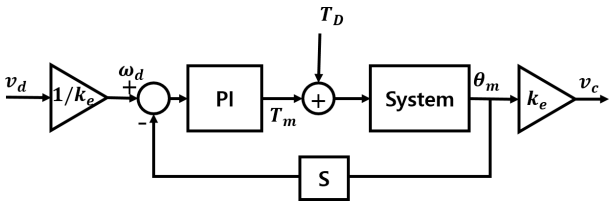

FIGURE 3. The low-level controller.

As shown in Figure 2(b), the system works to equalize the interaction and target forces ($F_{interaction}$ and $F_{desired}$, respectively) when operating in the force mode by generating the v_c that delivers a constant force to the user. Figure 4 shows

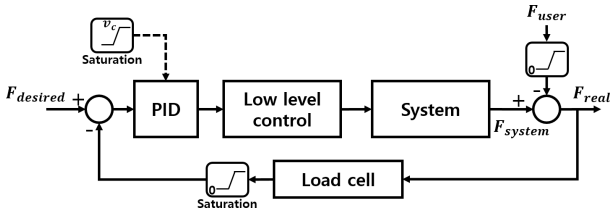

FIGURE 4. Block diagram of the force mode controller.

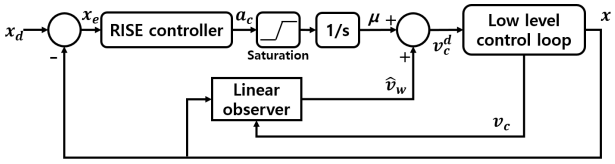

FIGURE 5. Block diagram of the distance mode controller.

a block diagram of the proportional-integral-derivative (PID) force mode controller that is used to apply $F_{desired}$ to the user independent of gait speed. The target of this closed-loop controller is to minimize the interaction force error ($F_{desired} - F_{interaction}$). The system velocity generated from the force error delivers a tensile force to the user (see Figure 2(b)). The $F_{interaction}$ between the user and system is measured using a force sensor. When the system interacts with the user, $F_{interaction}$ is the difference between the force generated by the system (F_{system}) and the force applied by the user (F_{user}). If the user applies an arbitrary force to the leash, the PID controller compensates for the change in load by increasing or decreasing the system's target velocity to maintain $F_{desired}$. Therefore, the system controls the relevant forces without measuring the user or system velocity. The saturation block (shown with a dotted line) shown in Figure 4 is only applied when the system is operated in the distance mode, and is excluded in the transition to force mode. This will be discussed further in Section II-F.

C. DESIGN OF THE DISTANCE MODE

The distance mode was designed to use a robust control scheme. In this mode, the distance between the robot and the user is maintained with no interaction forces between them; i.e., the robot should reach the desired distance from the user, x_d, and then match the user's velocity, v_w, as shown in Figure 2(a). The implemented control scheme is similar to that of a self-paced treadmill in which the velocity of the belt is matched to the user's velocity [39]. The user's initial gait speed was estimated with a robust integral of the sign of the error (RISE) controller and a low-gain observer. The RISE controller is a feedback control system; thus, the positional error was reduced by estimation of the time-varying uncertainty of the closed-loop system [40]. The low-gain observer was used as the feedforward term to estimate the user's gait speed at low acceleration. Through implementation of this method, the system can be made more comfortable by smoothing the rapid changes in velocity.

According to Figure 2(b), the user-system interaction state space model can be represented as follows [41]:

$$\dot{x} = -v_c + v_w \tag{1}$$

$$\dot{v_c} = a_c \tag{2}$$

where, x_e is the user position error, v_w represents the intentional velocity of the user, and v_c and a_c represent system velocity and acceleration, respectively. According to equation (1), v_c is the direct current (DC) motor driver control input from the low-level controller. However, as described in Ref. [41], equation (1) can be modified with equation (2) such that a_c is used as the input to prevent a large acceleration during system movement. The control command v_c can be obtained by integrating a_c.

The controller's objective is to reduce x_e to zero. Here, a positional error variable and its dynamics must be derived.

The desired controller output is calculated as follows:

$$v_c^d(t) = \hat{v}_w + \mu \tag{3}$$

where v_c^d is the desired velocity command, and $\hat{v}_w$ is a feedforward term that is an estimate of v_w that can be obtained from the linear observer [41]. The robust term μ is a continuous input, which includes the RISE controller, defined in Ref. [40] as follows:

$$\mu = (k_s + 1)\, x - (k_s + 1)\, x(0) + \int_0^t \left[(k_s + 1)\,\alpha_1 x + \beta \mathrm{sgn}(x)\right] d\bar{t} \tag{4}$$

where k_s, α_1, α_2 and β are adjustable positive control gains, and 'sgn' represents the standard sign function. The RISE controller learns the slowly time-varying uncertainties of the close-loop dynamic system, which compensates for the estimation error of the feedforward controller.

The error signal is defined as $q = v_c - v_c^d$. We assume that the low-level control can accurately follow target commands. Therefore, the dynamic model can be written as follows:

$$\dot{q} = 0 = a_c - \dot{v_w} - (k_s + 1)(v_w - v_c) - (k_s + 1)\,\alpha_1 x - \beta sgn(x) \tag{5}$$

With a_c as its input, a controller for (5) can be described by

$$a_c = \dot{v_w} + (k_s + 1)(v_w - v_c) + (k_s + 1)\,\alpha_1 x + \beta sgn(x) \tag{6}$$

This controller includes the terms v_w and $\dot{\hat{v}}_w$, which cannot be directly measured. However, the velocity is the system input command, so it can be obtained from $v_c(t) = \int_0^t a_c(\bar{t})\, d\bar{t}$. Thus, the final control command is approximated as follows:

$$v_c = \hat{v}_w + \beta \int_0^t sgn\left(x(\bar{t})\right) d\bar{t} + (k_s + 1) \int_0^t \left[\hat{v}_w(\bar{t}) - v_c(\bar{t}) + \alpha_1 x(\bar{t})\right] d\bar{t} \tag{7}$$

D. SYSTEM HARDWARE

The haptic companion robot shown in Figure 1(b) was controlled by an onboard controller and a motor driver was used to control the DC motor that powered the wheels; the system was supplied by a battery-powered switched-mode power supply (SMPS). A LIDAR sensor (TF Mini) was used to measure the distance between the robot and the user, and a load cell was used to measure the interaction force. The trailing caster wheel provided stability and enabled the robot to be turned freely in any direction. Detailed hardware specifications are provided in Table 1.

TABLE 1. The system specifications.

System	Max. velocity	1.5 m/s
	Weight	7.5 kg
	Size	180 x 180 x 1300 mm
Sensors	Load cell	CDES (Bongshin Loadcell Co.) Operating range: 100 kg, frequency: 50 Hz
	LIDAR	TF Mini LIDAR, operating range: 0.3-12 m Frequency: 100 Hz Light sensitivity: 70,000 lux accuracy: 1% (less than 6 m, independent of ambient lighting conditions)
Parts	Controller board	sbRIO-9636 (National Instruments Corp.)
	Motor	IG-52GM, power: 48.6W, gear ratio 19:1
	Motor Driver	Escon 50/5 (Maxon Motor AG)
	Battery	Lithium-ion (Samsung) 22.2V, 13,000mAh
	SMPS	GMS200, DC-DC 200W
	Wi-fi	ipTIME, IEEE 802.11n, 300 Mbps, 5 dBi

High-level control was executed using a laptop computer, which was also used for data logging. The laptop and mobile robot communicated via a WiFi (TCP/IP) link with a 1-kHz data rate (see Figure 6). For safety reasons, the software interface included an emergency stop button for use by the operator.

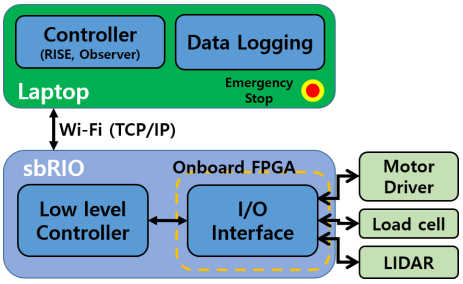

FIGURE 6. High-level block diagram of the system.

E. OPERATIONAL VERIFICATION OF THE DISTANCE AND FORCE MODES

Operational verification tests of the system were carried out outdoors with a single healthy user. First, the force mode was tested by applying a force between 2.5 and 10 N while, from a standing start, the user walked for 30 s. As shown in Figure 7, the maximum force fluctuation was not more than 2.5 N, which shows that the system can apply force in 2.5 N increments.

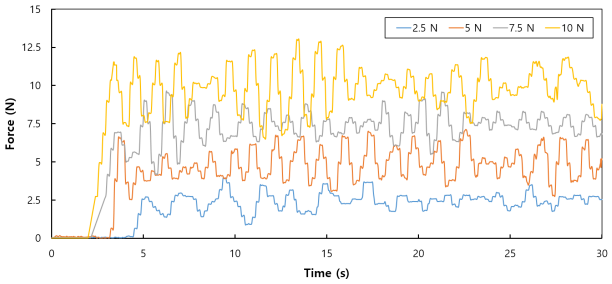

FIGURE 7. The interaction force values measured during the force mode trials.

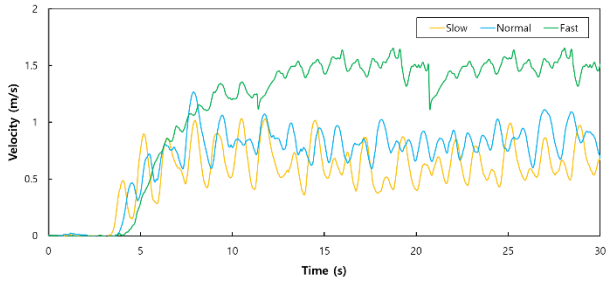

(a) The system velocities measured during the distance mode trials.

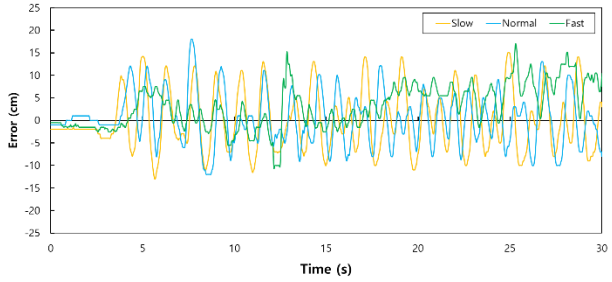

(b) The positional errors recorded during the distance mode trials.

FIGURE 8. The results of the distance mode trials.

The distance mode was tested by asking the user to walk with the system at a slow, normal, and fast pace. As shown in Figure 8, the average velocities for these three trials were 0.63, 0.81, and 1.33 m/s, respectively. The target distance for this test was set as 70 cm. The root mean square (RMS) errors of the distance between the device and user were 6.68, 5.76, and 5.77 cm, respectively, and the maximum error was 18.07 cm. The minimum safe distance between the user's COM and the device is 40 cm. Thus, the maximum acceptable amount of error in distance maintenance is 70 – 40 = 30 cm. Hence, these results demonstrate that the distance error was acceptably small and did not show any relationship with walking speed.

Thus, the system was shown to operate with acceptable accuracy in both force and distance modes. In the force mode, up to 10 N could be applied to the hand-held leash in the direction of motion. In the distance mode, no force

was applied through the leash, but the specified distance was maintained with a maximum user velocity of 1.5 m/s.

F. MODE TRANSITION ALGORITHMS

The system was programmed so that it was possible to apply a force for a programmed duration at any time during operation. This functionality required that the system could make automatic transitions between the distance and force modes. Safe operation required that these transitions did not pose any risk of an abrupt halt of the robot, or collision with the user. Furthermore, these transitions needed to be gradual so that the user did not feel compelled to make sudden gait adjustments as the system switched modes. Figures 9(a) and 9(b) illustrate the mode transition concepts that were implemented. The transitions were performed smoothly and safely using custom-designed algorithms, as described in Figure 9(c).

To transition from the distance to force mode, the robot must accelerate to reduce the slack in the leash, and then apply a leading force. The system is driven by the RISE and PID controllers when in the distance and force modes, respectively. Both controllers are kept in operation at all times to ensure smooth operation of the robot. In the distance mode, to ensure that only the RISE controller controls the system, the PID controller output is nullified by feeding the current system velocity back as the output saturation value (see Figure 9(c)). This output saturation is removed when a transition to the PID controller is initiated, which allows the PID output to increase and accelerate the robot. As the system accelerates, the distance between the user and robot increases to above the reference position value, which drives the RISE controller output to zero so that the PID controller output is the only non-zero motor control signal. This process is described pictorially in Figure 9(c).

During the transition from the force to distance mode, as shown in Figure 9(b), the device must decelerate to slacken the leash and remove the interaction force. During this transition, the user-robot separation is greater than that required in the distance mode, x_{ID} (set initially as the desired distance). Therefore, the robot stops abruptly to wait for the user to reach the reference position. Because the system stops, the user may also have to stop and wait for the robot to move again. The device may also become unstable due to the large x_e and user intentional velocity $\widehat{h_w}$.

The system makes this transition more gradual by measuring the average distance from the user during the first half of the last second of the force mode; this is the device's measured distance value, x_m. During the following 5 s (i.e., the first 5 s of the distance mode), the device linearly reduces the distance between itself and the user from the measured distance to the initial distance ($x_m \rightarrow x_{ID}$). The initial distance is the separation that was maintained between the device and user during the previous distance mode operation. This gradual reduction in distance removes the tension from the leash and ensures continuous motion of the device. The transition process is described in Figure 9(c), and the effects

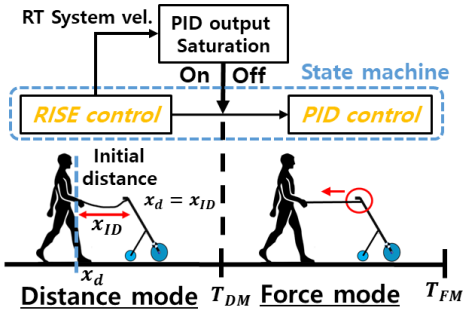

(a) The transition from distance to force mode.

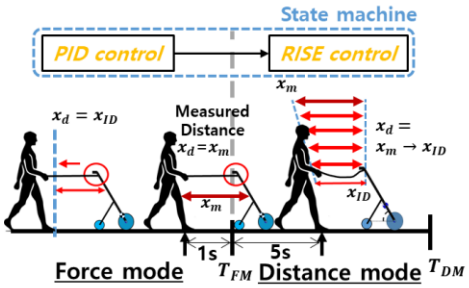

(b) The transition from force to distance mode.

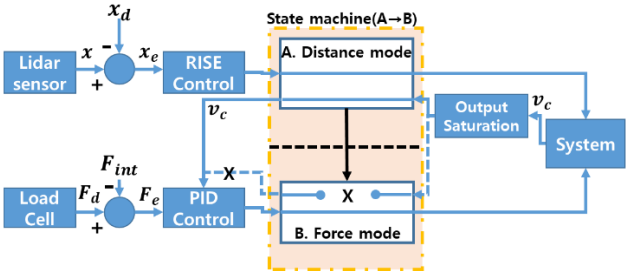

(c) Flowchart of the transition from distance to force mode.

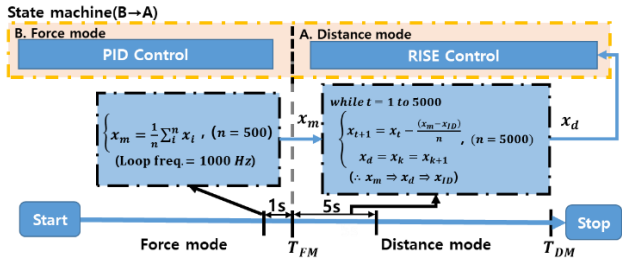

(d) Flowchart of the transition from force to distance mode.

FIGURE 9. The operation mode transitions (T_{DM} = duration of distance mode, T_{FM} = duration of force mode, x_d = desired position, x_{ID} = initial distance, x_m = average distance measured, n & k = the number of loop iterations).

of these transition algorithms are shown in Figures 11 and 12 and discussed further in Section IV.

III. EXPERIMENT

A pilot study was carried out in which the gait of six healthy, young subjects, and one individual who was recovering from a hemiparetic stroke was studied while they used our system. The primary focus of the study was to observe the

changes in user gait velocity when a haptic force was applied through the leash and then removed. Furthermore, we aimed to determine whether the introduction of a force changed user gait velocity, and how much time the user would require to return to their pre-force velocity. Our prototype device and the system developed by Sorrento *et al.* [22] operate on the same principles, so the experimental protocol used in Ref. [22] was adapted to include overground walking instead of treadmill walking, and different timings and force magnitudes. The six young, healthy participants (gender: male, mean age: 28.2 ± 4.7 years, mean height: 172.7 ± 3.0 cm, mean weight: 68.6 ± 16.6 kg) had no prior history of musculoskeletal or neurological injuries. The system is designed for people capable of unassisted locomotion, so the participant who was recovering from a hemiparetic stroke was selected accordingly (gender: female, age: 60 years, height: 148 cm, weight: 48 kg, right-sided hemiplegia, 22 days since onset, cause of stroke: infarction, Brunnstrom stages of stroke recovery: 4/4/5, modified Barthel index score: 44, mini-mental state exam (MMSE) score: above 24). All participants gave written informed consent prior to participation in the study.

A. PROTOCOL

All subjects followed the same walking trial protocol. First, the participants were introduced to the system and its functionality. The testing protocol was explained verbally, and the users were instructed to release the system if they felt unstable or uncomfortable. The users then underwent familiarity training which included walking with the system in both distance and force modes, and the transitions between them.

Once familiar with the device, each participant was subjected to two iterations of normal-walking and with-device-walking trials. In the normal-walking trial, the user walked in a straight line at their preferred gait speed for 14 m; each user's walk during the middle 10 m was timed using a stopwatch, and observations made during this period were used for data analysis.

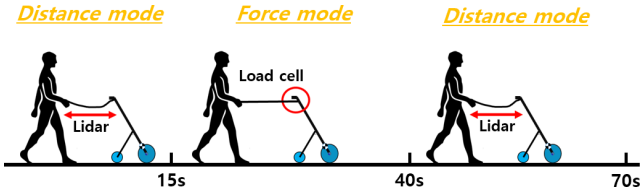

FIGURE 10. An illustration of the with-device-walking test protocol.

As shown in Figure 10, the with-device-walking trial required the subject to walk with the system for 70 s. During the first 15 s of the trial, the system led the user at their desired speed (distance mode), and the leash remained slack. Then the system automatically transitioned (distance to force mode transition) and for the next 25 s (including transition time), the system applied a force to the user's hand (force mode). At 40 s from the start of the trial, the system automatically transitioned (force to distance mode transition) and during the last 30 s (including transition time) it again led the user at their preferred speed (distance mode), such that the leash was slack. A 5-N haptic force was maintained throughout the force mode during all trials. The healthy subjects completed the with-device-walking trials in a 100-m-long hallway, whereas the individual with stroke performed the test in a 60-m-long hallway. All subjects were allowed to sit for 5 min between trials.

B. DATA COLLECTION AND ANALYSIS

The device velocity was calculated in real-time using the output of the optical encoder (which was used for low-level device control), and data were stored on the laptop for post-experimental analysis.

The interaction force between the user and the device was measured using the installed force sensor, and the haptic force felt by the user in the direction of motion is the horizontal component of this measured force. The time-dependent interaction force was also logged using the laptop.

During the with-device-walking trials, an experimental supervisor walked two paces behind the subject and placed markers on the ground 15, 40, and 70 s after the start of the trial to mark the distance travelled by the subject. After each trial, these distances were recorded. The distance and time information were used to calculate the gait speed of the subjects during each of the periods that corresponded to the three with-device-walking conditions (pre-force distance mode, force mode, and post-force distance mode). Data from the first 2 m of each trial were not considered during analysis.

All subjects wore shoes with instrumented insoles (Moticon, ReGo AG) that were used to measure the number of steps taken during each trial. This value and the distance travelled in each phase were used to estimate the step length of the subject for each device control mode.

A one-way repeated-measures analysis of variance (RMANOVA) was used to identify the effect of different walking modes on the gait speed and step length of the young, healthy subjects. Furthermore, Mauchly's test of Sphericity was used to confirm the validity of the RMANOVA results and post-hoc tests were carried out. All statistical analyses were performed using SPSS V20.0 (IBM Corp., Armonk, NY, USA).

IV. RESULTS AND DISCUSSION

A. HEALTHY SUBJECTS

The system velocity and interaction force during the with-device-walking trial of a single healthy subject are shown in Figures 11 and 12.

As shown in Figure 11, the user comfortably reached their preferred gait speed during the first 15 s of the trial (pre-force distance mode) and maintained it while walking with the device. During the following 25 s (force mode), the user increased their gait speed when the haptic force was applied through the leash and maintained this greater speed.

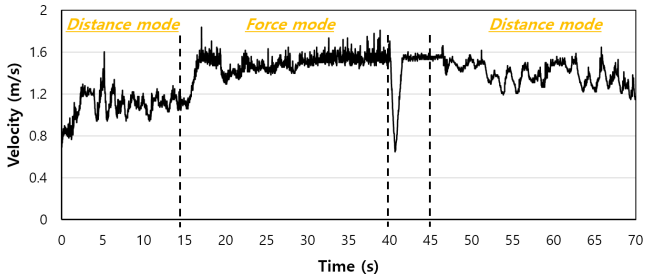

FIGURE 11. The system velocity during the with-device-walking trial of a representative healthy subject.

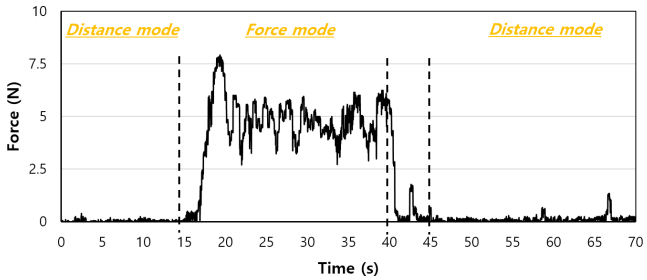

FIGURE 12. The interaction force received by a representative healthy subject during the with-device-walking trial.

The system decreased its velocity and transitioned from the force mode to the distance mode during the 5-s time period starting at 40 s into the trial. At this time, the device slackened the leash and reduced the haptic force by reducing its speed. This transition was carried out according to the algorithm described in Section II-F such that there were no abrupt changes in speed so severe that they may cause the user to trip over or collide with the system. Although at the start of the force to distance mode transition there is a drop in speed, it is very quickly recovered, and during trials none of the participants felt that this drop was a cause of disturbance for them. Upon removal of the force, the user's gait speed started to decrease slowly. At the end of the 70-s trial period, the user was nearing their preferred gait speed.

The interaction force experienced by a user during the with-device-walking trial is shown in Figure 12, which illustrates that the user walked with the system without any interaction force during the distance-mode periods, and only experienced the set 5-N interaction force during the force-mode phase.

The mean and standard deviation (SD) of the healthy subjects' velocities during the normal-walking and with-device-walking trials are shown in Figure 13. The users' gait speeds during the normal-walking and pre-force distance modes were not significantly different, which indicates that the system did not hinder the user when operating in distance mode. The application of the haptic force delivered by the leash increased the mean gait speed, and a corresponding decrease in mean gait speed was observed after the force was removed.

One-way RMANOVA revealed that the differences in gait speeds of the young, healthy subjects among the different

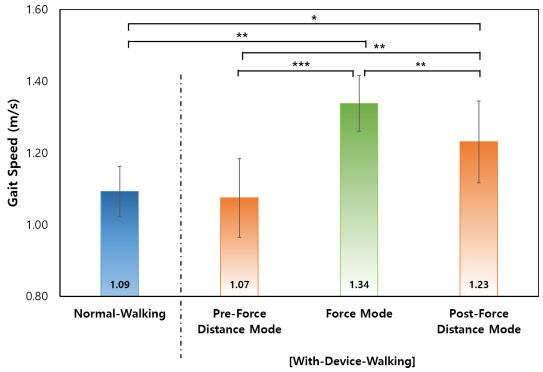

FIGURE 13. The mean gait speeds of all the healthy subjects measured during different walking modes. (* = p-value < 0.05,** = p-value < 0.02,*** = p-value < 0.001).

walking modes were statistically significant. ($F(3, 15) = 22.101$, P-value < 0.001). Post hoc tests showed that the gait speed was significantly greater during the force (P-value $= 0.002$) and post-force modes (P-value $= 0.027$) compared to the subjects' normal walking speeds. Likewise, the pre-force distance-mode gait speed was significantly different from the force (P-value < 0.001) and post-force distance-mode speeds (P-value $= 0.001$). The young, healthy subjects exhibited a statistically significant decrease in gait speed during the post-force distance mode compared to the force mode (P-value $= 0.002$).

The changes in gait speed observed during the with-device-walking trials agree with the findings of Sorrento *et al.* [22]. Furthermore, we verified that the use of our system in pre-force distance mode does not interfere with the user's preferred overground gait speed. The maximum difference in gait speeds between normal walking and the pre-force distance mode was 0.18 m/s, and the minimum was –0.01 m/s. This signifies that the current system is an appropriate source of on-demand force interaction.

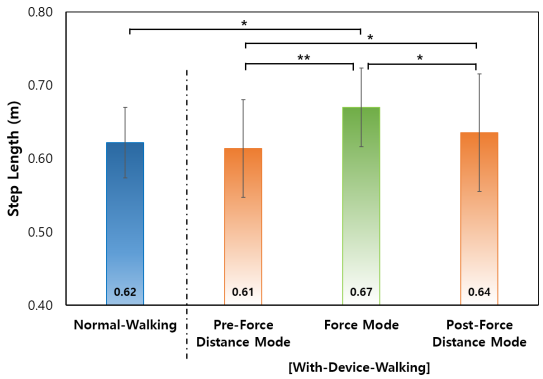

FIGURE 14. Mean values of the healthy subjects' step lengths in different walking modes. (* = p-value < 0.05,** = p-value < 0.02,*** = p-value < 0.001).

The step lengths estimated during the normal-walking and with-device-walking trials are shown in Figure 14. The increase in step length following the application of a haptic

force can be attributed to the immediate increase in user gait speed. Similarly, the decrease in step length following the removal of force can be attributed to the decrease in gait speed. One-way RMANOVA revealed that the step length of the young healthy subjects differed significantly among different walking modes ($F(3, 15) = 4.476$, P-value $= 0.020$). Post-hoc tests revealed that step length increased significantly during the force-mode phase relative to normal-walking ($P = 0.046$). Similarly, the pre-force distance-mode step length was significantly different from those measured during the force (P-value < 0.009) and post-force distance modes (P-value $= 0.039$). Furthermore, young, healthy subjects exhibited a statistically significant decrease in step length in the post-force phase compared to that during the force mode (P-value $= 0.043$). The changes in step length observed during the with-device-walking trials are also consistent with the findings of Sorrento *et al.* [22].

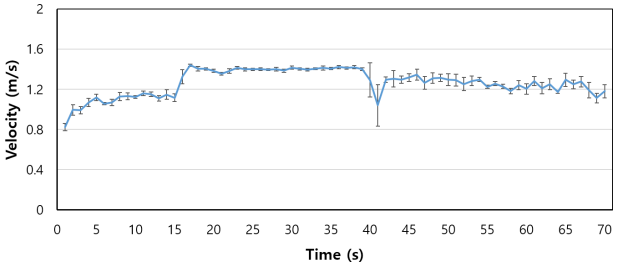

FIGURE 15. Mean system velocity during the with-device-walking trials of all young, healthy subjects.

The mean system velocity of all healthy subjects during the with-device-walking trials, averaged over 1-s intervals, is shown in Figure 15. An increase in the mean system velocity represents an increase in the gait speed of the user following the application of force. These data show that upon removal of the force, the users' gait speeds tended to revert back to the pre-force distance mode gait speed over an extended period. We hypothesized that users would require a similar amount of time to revert to their preferred gait speed after experiencing an increase in gait speed due to the application of force for 25 s. The time-dependent velocity time-series revealed that user gait speed decreased between 45 and 70 s (Figure 15). This trend is in agreement with our hypothesis, but the time required to return to the pre-force gait speed may be greater than we expected. Further study is required to find a correlation between the duration of force application and the time required for a user to return to their preferred gait velocity.

B. INDIVIDUAL RECOVERING FROM A STROKE

Based on the observations made during the trials with healthy subjects, a pilot trial was carried out with an individual suffering from hemiparesis following a stroke to examine the effects of our prototype device. We used the same protocol, with the addition of a therapist walking a couple of paces behind the subject to ensure their safety. The gait speed and step length of the subject during normal-walking and with-device-walking trials exhibited trends similar to those observed with young, healthy subjects.

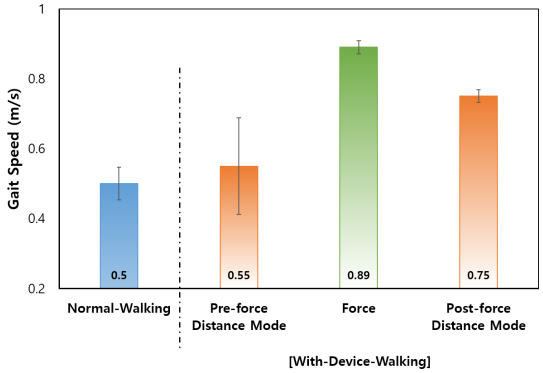

FIGURE 16. Mean gait speed of the subject recovering from a stroke during each trial phase.

Figure 16 shows the gait speed of the individual recovering from a stroke during normal-walking and with-device-walking trials. As observed with the healthy subjects, the gait speeds during normal-walking and the pre-force distance modes were not significantly different. Following the application of a 5-N haptic force during the force mode, an increase in gait speed was observed, and a decrease was seen upon removal of the force.

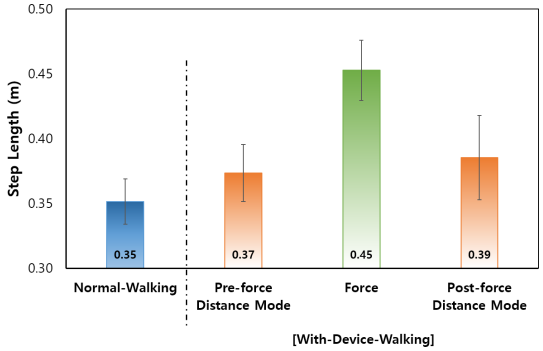

FIGURE 17. Mean step length of the subject recovering from a stroke during each trial phase.

Figure 17 shows the subject's step length during the trials. The changes in step length may have resulted from the changes in gait speed associated with the introduction of the haptic force.

Changes in gait speed and step length indicate that the individual had adapted their gait to changes in system modes. Although only short-duration adaptations were tested in this work, these results indicate that long-term adaptations may occur through the implementation of extended training protocols.

V. CONCLUSION AND FUTURE WORK

We have presented the development of a companion robot system that provides haptic interaction, which may be a useful tool for overground gait rehabilitation of individuals with stroke who are in the chronic stage of recovery and are capable of walking stably without any assistance. This system emulates the interactions between a human and a

dog on a leash that may be useful for facilitating gait recovery while eliminating the unpredictable behaviors associated with live animals. This system, unlike those in previous studies [22], does not require the use of a treadmill, which increases accessibility for outpatients who need to continue their overground rehabilitation. The trends in gait speed and step length observed during the trials involving healthy subjects are consistent with the observations of researchers that have explored the use of real and virtual companion animals for gait recovery [22], [29]. Furthermore, experimental observations demonstrated that the system presented here did not have a significant influence on the user's gait when no force was applied (distance mode). Overall, the findings presented here show that this system can be used as a robotic companion for gait rehabilitation.

The tilted-cane portable robot was designed to have a flexible linkage to the user, allowing for the total elimination of force interaction when desired. It can move at a wide range of speeds and generate a range of interaction forces, which makes it suitable for many users' needs. The patient found the system easy to use and exhibited gait speed and step length behaviors that were similar to those of healthy subjects.

The increase in gait speed observed after a haptic force was applied declined once the force was removed. This suggests that further study of the correlation between the force application duration and the time required for the gait speed to return to the user's preferred speed may be required. Furthermore, the effects of different haptic-force loads should be investigated in addition to the effects of long-term training as a means of instilling more permanent gait adaptations.

This study assessed the performance of six young, healthy subjects, and one individual recovering from a stroke. All participants demonstrated outcomes that were consistent with the observations of previous researchers. Further studies comprising comprehensive gait analysis, including kinematic and postural measures to evaluate the system's effects on individuals who have suffered a stroke need to be conducted to further explore the device's potential as a tool for gait rehabilitation.

Certain design changes are required to enable this system to be used in an outdoor setting. The system track width is narrow, which provides high maneuverability, but may make the system unstable on uneven surfaces such as those encountered outdoors. The system does not have powered direction control or obstacle detection and avoidance functions [42], which may aid outdoor operations. An update to the system design would improve the robustness of the system for outdoor use and may enable the implementation of outdoor training protocols that are closer to the users' real-life environments.

REFERENCES

[1] S. E. Lord and L. Rochester, "Measurement of community ambulation after stroke," *Stroke*, vol. 36, no. 7, pp. 1457–1461, Jul. 2005.

[2] C. S. Nanninga, L. Meijering, K. Postema, M. C. Schönherr, and A. T. Lettinga, "Unpacking community mobility: A preliminary study into the embodied experiences of stroke survivors," *Disab. Rehabil.*, vol. 40, no. 17, pp. 2015–2024, Aug. 2018.

[3] M. Y. Pang, J. J. Eng, and W. C. Miller, "Determinants of satisfaction with community reintegration in older adults with chronic stroke: Role of balance self-efficacy," *Phys. Therapy*, vol. 87, no. 3, pp. 282–291, Mar. 2007.

[4] R. W. Bohannon, M. G. Morton, and J. B. Wikholm, "Importance of four variables of walking to patients with stroke," *Int. J. Rehabil. Res.*, vol. 14, no. 3, pp. 246–250, Sep. 1991.

[5] L. A. Malone, E. V. L. Vasudevan, and A. J. Bastian, "Motor adaptation training for faster relearning," *J. Neurosci.*, vol. 31, no. 42, pp. 15136–15143, Oct. 2011.

[6] C. J. Wutzke, V. S. Mercer, and M. D. Lewek, "Influence of lower extremity sensory function on locomotor adaptation following stroke: A review," *Topics Stroke Rehabil.*, vol. 20, no. 3, pp. 233–240, May 2013.

[7] D. S. Reisman, R. Wityk, K. Silver, and A. J. Bastian, "Split-belt treadmill adaptation transfers to overground walking in persons poststroke," *Neurorehabil. Neural Repair*, vol. 23, no. 7, pp. 735–744, Sep. 2009.

[8] D. N. Savin, S. M. Morton, and J. Whitall, "Generalization of improved step length symmetry from treadmill to overground walking in persons with stroke and hemiparesis," *Clin. Neurophysiol.*, vol. 125, no. 5, pp. 1012–1020, May 2014.

[9] J. W. Krakauer, "Adaptation to visuomotor transformations: Consolidation, interference, and forgetting," *J. Neuroscience*, vol. 25, no. 2, pp. 473–478, Jan. 2005.

[10] R. A. States, Y. Salem, and E. Pappas, "Overground gait training for individuals with chronic stroke: A cochrane systematic review," *J. Neurol. Phys. Therapy*, vol. 33, no. 4, pp. 179–186, Dec. 2009.

[11] M. An and M. Shaughnessy, "The effects of exercise-based rehabilitation on balance and gait for stroke patients," *J. Neurosci. Nursing*, vol. 43, no. 6, pp. 298–307, Dec. 2011.

[12] J. Hidler, D. Nichols, M. Pelliccio, K. Brady, D. D. Campbell, J. H. Kahn, and T. G. Hornby, "Multicenter randomized clinical trial evaluating the effectiveness of the Lokomat in subacute stroke," *Neurorehabil Neural Repair*, vol. 23, no. 1, pp. 5–13, Jan. 2009.

[13] P. M. Davies, *Right in the Middle: Selective Trunk Activity in the Treatment of Adult Hemiplegia*. Berlin, Germany: Springer-Verlag, 1990.

[14] P. M. Davies, *Steps to Follow: The Comprehensive Treatment of Patients With Hemiplegia*, 2nd ed. Berlin, Germany: Springer-Verlag, 2000.

[15] B. E. B. Gjelsvik, *The Bobath Concept in Adult Neurology*. Stuttgart, Germany: Georg Thieme Verlag, 2008.

[16] R. F. Macko, F. M. Ivey, L. W. Forrester, D. Hanley, J. D. Sorkin, L. I. Katzel, K. H. Silver, and A. P. Goldberg, "Treadmill exercise rehabilitation improves ambulatory function and cardiovascular fitness in patients with chronic stroke," *Stroke*, vol. 36, no. 10, pp. 2206–2211, Oct. 2005.

[17] A. M. Moseley, A. Stark, I. D. Cameron, and A. Pollock, "Treadmill training and body weight support for walking after stroke," *Stroke*, vol. 34, no. 12, p. 3006, Dec. 2003.

[18] C. Werner, A. Bardeleben, K.-H. Mauritz, S. Kirker, and S. Hesse, "Treadmill training with partial body weight support and physiotherapy in stroke patients: A preliminary comparison," *Eur. J. Neurol.*, vol. 9, no. 6, pp. 639–644, Nov. 2002.

[19] L. Turchet, S. Serafin, and P. Cesari, "Walking pace affected by interactive sounds simulating stepping on different terrains," *ACM Trans. Appl. Percept.*, vol. 10, no. 4, pp. 1–14, Oct. 2013.

[20] J. M. Finley, M. A. Statton, and A. J. Bastian, "A novel optic flow pattern speeds split-belt locomotor adaptation," *J. Neurophysiol.*, vol. 111, no. 5, pp. 969–976, Mar. 2014.

[21] G. Torres-Oviedo and A. J. Bastian, "Seeing is believing: Effects of visual contextual cues on learning and transfer of locomotor adaptation," *J. Neurosci.*, vol. 30, no. 50, pp. 17015–17022, Dec. 2010.

[22] G. U. Sorrento, P. S. Archambault, and J. Fung, "Adaptation and post-adaptation effects of haptic forces on locomotion in healthy young adults," *J. NeuroEng. Rehabil.*, vol. 15, no. 1, Dec. 2018.

[23] M. Roerdink, C. J. Lamoth, G. Kwakkel, P. C. van Wieringen, and P. J. Beek, "Gait coordination after stroke: Benefits of acoustically paced treadmill walking," *Phys. Therapy*, vol. 87, no. 8, pp. 1009–1022, Aug. 2007.

[24] M. Afzal, H.-Y. Byun, M.-K. Oh, and J. Yoon, "Effects of kinesthetic haptic feedback on standing stability of young healthy subjects and stroke patients," *J. NeuroEng. Rehabil.*, vol. 12, no. 1, p. 27, 2015.

[25] R. Dickstein and Y. Laufer, "Light touch and center of mass stability during treadmill locomotion," *Gait Posture*, vol. 20, no. 1, pp. 41–47, Aug. 2004.
[26] E. Kodesh, F. Falash, E. Sprecher, and R. Dickstein, "Light touch and medio-lateral postural stability during short distance gait," *Neurosci. Lett.*, vol. 584, pp. 378–381, Jan. 2015.
[27] J. J. Jeka and J. R. Lackner, "Fingertip contact influences human postural control," *Exp. Brain Res.*, vol. 100, no. 3, pp. 495–502, Aug. 1994.
[28] M. R. Afzal, A. Eizad, C. E. Palo Peña, and J. Yoon, "Evaluating the effects of kinesthetic biofeedback delivered using reaction wheels on standing balance," *J. Healthcare Eng.*, vol. 2018, pp. 1–10, Jun. 2018.
[29] L. Rondeau, H. Corriveau, N. Bier, C. Camden, N. Champagne, and C. Dion, "Effectiveness of a rehabilitation dog in fostering gait retraining for adults with a recent stroke: A multiple single-case study," *NeuroRehabilitation*, vol. 27, no. 2, pp. 155–163, Sep. 2010.
[30] E. Rabin, A. Demin, S. Pirrotta, J. Chen, H. Patel, A. Bhambri, E. Noyola, J. R. Lackner, P. DiZio, J. DiFrancisco-Donoghue, and W. Werner, "Parkinsonian gait ameliorated with a moving handrail, not with a banister," *Arch. Phys. Med. Rehabil.*, vol. 96, no. 4, pp. 735–741, Apr. 2015.
[31] A. A. D. S. Costa, P. A. R. Manciopi, E. Mauerberg-deCastro, and R. Moraes, "Haptic information provided by the 'anchor system' reduces trunk sway acceleration in the frontal plane during tandem walking in older adults," *Neurosci. Lett.*, vol. 609, pp. 1–6, Nov. 2015.
[32] E. V. Lamont and E. P. Zehr, "Earth-referenced handrail contact facilitates interlimb cutaneous reflexes during locomotion," *J. Neurophysiol.*, vol. 98, no. 1, pp. 433–442, Jul. 2007.
[33] J. Fung and C. F. Perez, "Sensorimotor enhancement with a mixed reality system for balance and mobility rehabilitation," in *Proc. Annu. Int. Conf. IEEE Eng. Med. Biol. Soc.*, Aug. 2011, pp. 6753–6757.
[34] F. Alton, L. Baldey, S. Caplan, and M. C. Morrissey, "A kinematic comparison of overground and treadmill walking," *Clin. Biomech.*, vol. 13, no. 6, pp. 434–440, Sep. 1998.
[35] J. Fung, C. L. Richards, F. Malouin, B. J. McFadyen, and A. Lamontagne, "A treadmill and motion coupled virtual reality system for gait training post-stroke," *CyberPsychol. Behav.*, vol. 9, no. 2, pp. 157–162, Apr. 2006.
[36] B. Brouwer, K. Parvataneni, and S. J. Olney, "A comparison of gait biomechanics and metabolic requirements of overground and treadmill walking in people with stroke," *Clin. Biomech.*, vol. 24, no. 9, pp. 729–734, Nov. 2009.
[37] I.-M. Park, Y.-S. Lee, B.-M. Moon, and S.-M. Sim, "A comparison of the effects of overground gait training and treadmill gait training according to stroke patients' gait velocity," *J. Phys. Theroy Sci.*, vol. 25, no. 4, pp. 379–382, 2013.
[38] S.-H. Pyo, M.-G. Oh, and J.-W. Yoon, "Development of an active haptic cane for gait rehabilitation," in *Proc. IEEE Int. Conf. Robot. Autom. (ICRA)*, May 2015, pp. 4464–4469.
[39] H. J. Asl, S.-H. Pyo, and J. Yoon, "An intelligent control scheme to facilitate abrupt stopping on self-adjustable treadmills," in *Proc. IEEE Int. Conf. Robot. Autom. (ICRA)*, May 2018, pp. 1639–1644.
[40] B. Xian, D. M. Dawson, M. S. de Queiroz, and J. Chen, "A continuous asymptotic tracking control strategy for uncertain nonlinear systems," *IEEE Trans. Autom. Control*, vol. 49, no. 7, p. 1206, Jul. 2004.
[41] J. L. Souman, P. R. Giordano, M. Schwaiger, I. Frissen, T. Thümmel, H. Ulbrich, A. D. Luca, H. H. Bülthoff, and M. O. Ernst, "CyberWalk," *ACM Trans. Appl. Percept.*, vol. 8, no. 4, pp. 1–22, Nov. 2011.
[42] D. Ni, A. Song, L. Tian, X. Xu, and D. Chen, "A walking assistant robotic system for the visually impaired based on computer vision and tactile perception," *Int. J. Social Robot.*, vol. 7, no. 5, pp. 617–628, Nov. 2015.

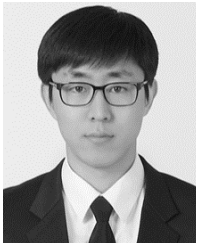

HOSU LEE received the B.E. degree in mechanical engineering and the M.S. degree in mechanical design degree from the School of Mechanical Engineering, Gyeongsang National University, Jinju, South Korea, in 2014 and 2016, respectively. He is currently pursuing the Ph.D. degree with the School of Integrated Technology, Gwangju Institute of Science and Technology, Gwangju, South Korea.

From 2016 to 2017, he joined as a Researcher and the Ph.D. student with Gyeongsang National University. In 2018, he joined the School of Integrated Technology, Gwangju Institute of Science and Technology. His current research interests include mechatronics, gait rehabilitation robots, and robot applications. He has also served as a Teaching Assistant with Gyeongsang National University, from 2016 to 2017.

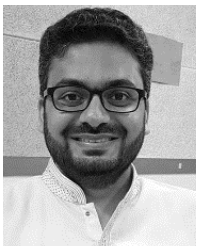

AMRE EIZAD was born in Peshawar, KPK, Pakistan, in 1987. He received the B.E. degree in mechatronics engineering and the M.S. degree in mechatronics engineering from Air University, Islamabad, Pakistan, in 2009 and 2011 respectively. He is currently pursuing the Ph.D. degree in mechanical engineering with Gyeongsang National University, Jinju, South Korea.

He has served as a Lab Engineer, from 2009 to 2011, and as a Lecturer, from 2011 to 2016, with the Department of Mechatronics Engineering, Air University. His research interest includes the development of robotic rehabilitation systems for people with neuromuscular disorders.

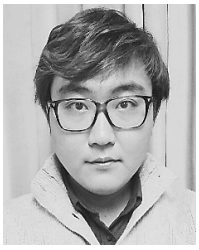

SANGHUN PYO received the B.A. and M.S. degrees from the School of Mechanical Engineering, Gyeongsang National University, Jinju, South Korea, in 2012 and 2014, respectively. He is currently pursuing the Ph.D. degree with the Gwangju Institute of Science and Technology (GIST).

He is also working on development of a stable gait interface controller on a 2-Dimensional treadmill and design of a 4DOF robot controller for user's trunk rehabilitation. His research interests include human–robot interaction and rehabilitation robot. In his career, he won the Excellence Prize by the theme of a knee support that can support walking in the Korea Invention Contest 2012.

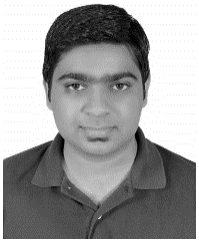

MUHAMMAD RAHEEL AFZAL was born in Islamabad, Pakistan, in 1989. He received the B.E. and M.S. degrees in mechatronics engineering from Air University, Islamabad, Pakistan, in 2010 and 2012, respectively, and the Ph.D. degree in mechanical and aerospace engineering from Gyeongsang National University, Jinju, South Korea, in 2018.

He worked as a Postdoctoral Researcher with the Intelligent Medical Robotics Laboratory, Gwangju Institute of Science and Technology, South Korea. Since January 2019, he has been with the Intelligent Mobile Platforms Research Group, KU Leuven, Belgium, where he currently works as a Research Team Lead. His current research interests include rehabilitation robotics, haptics, and mobile robotics.

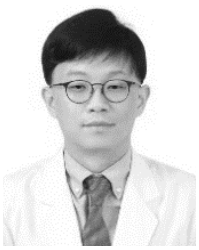

MIN-KYUN OH was born in Pusan, South Korea, in 1971. He received the B.S. and M.S. degrees and the Ph.D. degree in medicine from the Gyeongsang National University School of Medicine, Jinju, South Korea.

From 2007 to 2008, he was a Clinical Lecturer with the Department of Rehabilitation Medicine, Seoul National University Bundang Hospital. Since 2008, he has been a Professor of rehabilitation medicine with Gyeongsang National University Hospital and School of Medicine. He is currently a member of the Editorial Board of the Korean Academy of Rehabilitation Medicine and the Board Member of the Korean Society of Neuro Rehabilitation.

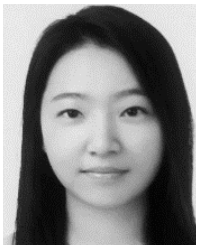

YUN-JEONG JANG was born in South Korea, in 1988. She received the B.S. and M.S. degrees in medicine from Gyeongsang National University, Jinju, South Korea, in 2011 and 2016, respectively.

She is currently working as a Resident with the Department of Rehabilitation Medicine, Gyeongsang National University School of Medicine and the Gyeongsang National University Hospital, Jinju. She is interested in gait training with prosthetics and orthotics.

JUNGWON YOON (Member, IEEE) received the Ph.D. degree from the Department of Mechatronics, Gwangju Institute of Science and Technology (GIST), Gwangju, South Korea, in 2005.

From 2005 to 2017, he was a Professor with the School of Mechanical and Aerospace Engineering, Gyeongsang National University, Jinju, South Korea. In 2017, he joined the School of Integrated Technology, Gwangju Institute of Science and Technology, Gwangju, South Korea, where he is currently an Associate Professor. He is also a Technical Editor of the IEEE/ASME TRANSACTIONS ON MECHATRONICS and an Associate Editor of *Frontiers in Robotics and AI*. He has authored or coauthored more than 80 peer-reviewed journal articles and patents. His current research interests include bio-nano robot control, virtual reality haptic devices, and rehabilitation robots.